Interaction Between MELK and EZH2 Regulates Medulloblastoma Cancer Stem-like Cells Proliferation

Hailong Liu; Qianwen Sun; Chunjiang Yu; Chunyu Gu; Hongwei Zhang

CNS 2017 ANNUAL MEETING
BOSTON, MASSACHUSETTS
OCTOBER 7–11, 2017

Introduction

Medulloblastoma (MB) is the most common malignant brain tumor in children. Although accumulated research suggests that cancer stem-like cells may play a key role in medullolastoma tumorigenesis, the molecular mechanisms of proliferation still remain elusive and further investigation can provide a novel application for therapeutic target in MB patients.

Methods

The expression of MELK and EZH2 was detected by tissue microarray analysis with 88 MBs and its association with prognosis was identified. Co-location of MELK and EZH2 in MB CSCs and tissues was studied by using confocal and immunostaining. Immunoblotting analysis following co-immunoprecipitation was performed to check the interaction between MELK and EZH2. Through the loss-of-function study by siRNA, CSCs-drived tumor growth was detected. Then we studied the targeted treatment of MB with MELK and EZH2 inhibitor in vivo to confirm the molecular basis of MELK and EZH2.

Results

MELK and EZH2 co-located in the nuclei of MB CSCs and MB with extensive nodularity and large cell/anaplastic differed the staining levels as measured using microarray analysis when compared with the other two subgroups. The proportion of MELK positive staining cells was the potential indicator for the survival. MELK bound and phosphorylated EZH2 and its methylation was induced by EZH2 in MB, which regulated the proliferation of CSCs. MELK and EZH2 depletion by siRNA or treatment of inhibitors attenuated the MB CSCs-derived tumor growth in vivo.

Conclusions

Interaction between MELK and EZH2 is essential for MB CSCs-drived tumor proliferation, thereby identifying a potential therapeutic strategy for MB patients.

Learning Objectives

To identify the important role of the interaction between MELK and EZH2 in medulloblastoma proliferation and then confirm a new advancing therapeutic

Figure.1

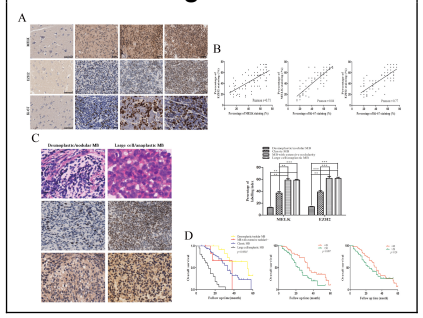

MELK and EZH2 protein were highly expressed in MB specimens. (A) Representative IHC images in low-magnifying fields (100×) showed that MELK, EZH2 and Ki-67 highly expressed in MB compared with normal brain tissues and the staining levels could be ranked in three grades. (B) MELK and EZH2 expression, as well as MELK or EZH2 and Ki-67 expression from 88 specimens were compared for their correlation. The Pearson correlation coefficients were 0.71, 0.86 and 0.77 respectively. (C) Left, epresentative images of MELK and EZH2 expression in desmoplastic/nodular and large cell/anaplastic subtypes of MB in low-magnifying fields (100×). The first line showed morphology in high-magnifying fields (H.E. 200×). Right, statistic graph showed that staining levels of MELK and EZH2 in large cell/anaplastic MB were significantly higher than that in other subtypes. ($p<0.01$; $p<0.0001$) (D) Left, The relationship between OS and histological subtypes was evaluated by Kaplan-Meier analysis indicating that patients with desmoplastic/nodular and classic subtypes had longer OS than the other two. ($p<0.0001$) Middle and right, patients were divided into two groups according to the MELK (middle) or EZH2 (right) expression levels and the postsurgical survival rate was evaluated by Kaplan-Meier analysis. There was a significant difference between the high MELK staining group and the low group, but the similar result wasn't obtained in EZH2 expression. ($p<0.01$; $P=0.26$)

Figure.2

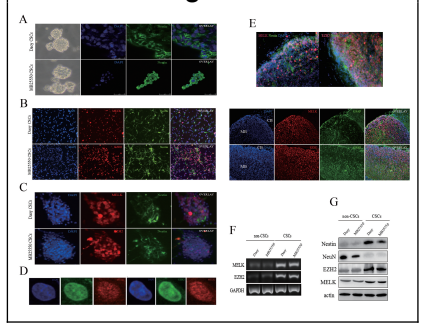

MELK and EZH2 protein co-located in MB CSCs. (A) Morphology of Daoy and MB25550 CSCs spheres was shown and both cell spheres were stained with Nestin. Bar=250 μm. (B) Dissociated Daoy and MB25550 CSCs binding dish were stained with MELK, EZH2 and Nestin showing that MELK or EZH2 was coexpressed with nestin (100×). (C) Immunocytochemistry of single Daoy and MB25550 spheres showed that MELK or EZH2 was coexpressed with nestin. Bar=500 μm. (D) Positively stained single cells showed that MELK and EZH2 co-located in the nuclei. Bar=5 μm. (E) Upper, immunostaining for MELK, EZH2 and GFAP of cerebellar sections of Ptc+/- mouse model at 12 weeks showed that MELK and EZH2 highly expressed in tumor lesions but not in normal cerebellum (100×). Lower, immunostaining for MELK, EZH2 and Nestin of xenograft sections at 4 weeks following transplantation with dissociated MB25550 CSCs showed that MELK and EZH2 highly expressed in tumor lesions and Nestin levels also increased (400×). (F) RT-PCR analysis displayed that MELK and EZH2 mRNA expression in CSCs were higher than that in non-CSCs. GAPDH was used as the internal control. (G) Western blotting analysis with Daoy and MB25550 showed that the expression of MELK, EZH2 and Nestin is higher in CSCs spheres compared with the differentiated progeny (non-CSCs), whereas NeuN expressed higher in non-CSCs. Actin was used as the internal control.

Figure.4

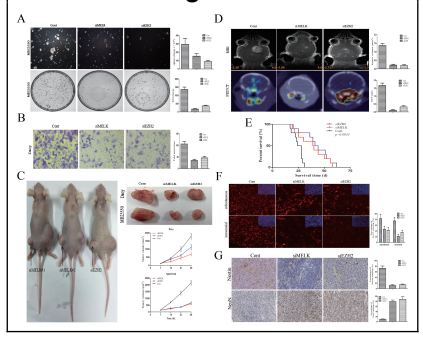

MELK or EZH2 knockdown attenuated MB CSCs proliferation. (A) MELK and EZH2 knockdown had significant inhibitory effects on the sphere and colony formation in MB25550 CSCs (100× and 10×).(B) Cell migration was evaluated by the transwell chamber assay without coated Matrigel displaying that differentiated Daoy cells transfected with plasmid carrying siMELK or siEZH2 had decreased mobility. The statistic graph showed the suppressed effects of siMELK and siEZH2 on migration compared with the control group. ($p<0.05$) (C) Daoy and MB25550 CSCs infected with lentiviral vector carrying shMELK (#1 and #2) or shEZH2 were subcutaneously transplanted into nude mice respectively and representative pictures were shown as the inhibitory effects on tumor growth.($p<0.05$; $p<0.01$) (D) MicroMRI scans (upper) for 3 distinct nude mice with intracranial tumors derived from stereotactic xenograft of MB25550 CSCs infected with lentiviral vector carrying shMELK#1 or shEZH2 on 28th day showed that MELK or EZH2 knockdown attenuated tumor growth. PET/CT (lower) on 28th day demonstrated the inhibitory effects on metastasis. The graph indicated the statistically evident difference of tumor volumes and radioactive absorptance. No -target shRNA was used as the control. ($p<0.0001$; $p<0.0001$) (E) Kaplan-Meier analysis indicated that mice bearing shMELK and shEZH2-infected MB25550 CSCs-derived intracranial tumors had a longer survival than the no-target control. ($p<0.01$) (F) Immunostaining for Ki-67 of shMELK- and shEZH2-transfected MB25550 CSCs-derived tumor sections displayed the elimination of proliferation by MELK or EZH2 knockdown compared with the on-target control (100×). The statistic graph showed the number of cells with Ki-67 positive staining. ($p<0.05$) (G) Representative IHC images of Nestin and NeuN staining in intracranial xenograft samples derived from no-target shRNA, shMELK and

Figure.3